

IMECE2009-12616

## BUBBLE DYNAMICS under FORCED OSCILLATION in MICROGRAVITY ENVIRONMENT

**Mohammad Movassat**

University of Toronto  
Mechanical and Industrial  
Engineering Department,  
Toronto, ON, Canada

**Nasser Ashgriz**

University of Toronto  
Mechanical and Industrial  
Engineering Department,  
Toronto, ON, Canada

**Markus Bussmann**

University of Toronto  
Mechanical and Industrial  
Engineering Department,  
Toronto, ON, Canada

### ABSTRACT

Two-dimensional numerical simulation of bubble dynamics in microgravity is performed employing a Volume of Fluid (VOF) solver. Shape oscillation and deformation of bubbles under forced vibration are studied. Coupling between the oscillatory translational motion and shape deformation results in nonlinear behavior of bubbles at high amplitudes and frequencies. As a result of oscillation of the buoyancy force, the pressure field around the bubbles oscillates and bubbles interact with each other. Effect of vibration frequency and amplitude and liquid to gas density ratio on the shape of bubbles and bubble-bubble interaction is studied. It is shown that the shape of the bubbles in response to the forced vibrations mainly depends on the acceleration of the vibration.

### INTRODUCTION

Gas bubbles in a liquid will respond to the pulsation of the surrounding pressure by volume oscillation, shape oscillation, or both. If the pressure variation is symmetric, bubbles will maintain a spherical shape, because of surface tension. If the amplitude of the surrounding pressure pulsation becomes sufficiently large, the spherical shape of the bubble becomes unstable. The slightest distortion in the shape then leads to shape oscillation [1]. In the case of a non-symmetric pressure oscillation, in addition to the shape oscillation, there will be a

translational motion depending on the direction of the pressure gradient. As a result of shape oscillation and oscillatory translational motion, a flow field develops around the bubble. In the case of more than one bubble, these flow fields interact with each other, resulting in bubble-bubble interaction.

Since the forces acting on a bubble depend on its shape and volume, there is a coupling between the change in the shape and volume of the bubble and its translational motion. For instance, shape changes change the pressure distribution on the interface and around the bubble, affecting the applied buoyancy force. Akhatov and Konovalova [2] studied the effect of this coupling on the behavior of a bubble suspended in a liquid medium using acoustic forces. Results suggested that at certain amplitudes and frequencies, bifurcation happens and the bubble movement turns chaotic. In their study, rather than solving the complete governing equations, simple models were employed to calculate bubble translational motion. The possibility of the chaotic behavior of bubbles in microgravity and under forced vibration has not been studied so far.

Bubble-bubble interaction can be observed when forces among bubbles are large compared to the gravitational buoyancy force. In the presence of gravity, an acoustic force can be employed to trap and levitate the bubbles. This force also results in a volume oscillation of the bubbles, which produces

pressure waves (i.e. interaction force) that affect other bubbles. The levitation force and interaction forces are called the primary and secondary Bjerknes forces [3], respectively. The volume oscillation of the bubbles is governed by the well-known Rayleigh-Plesset equation [4]. The results of studies in acoustic fields showed that the type of interaction between bubbles (attraction/repulsion) depends on fluid properties, bubble size, distance between bubbles, and pressure oscillation amplitude and frequency [5]. Microgravity provides an appropriate environment to study bubble dynamics. Most of the studies conducted so far have been confined to the behavior of a single bubble in microgravity under forced vibration. A good summary can be found in the work of Friesen [6]. These studies showed that the bubble shows an oscillatory translational motion with the same frequency as that of the vibrated cell and the amplitude of the bubble oscillation varies linearly with the amplitude of the cell vibration. In addition to an oscillatory translational motion, a net drift of the bubble was reported which was interpreted as the effect of adjacent solid boundaries.

This work presents a numerical study on the behavior of a pair of bubbles enclosed in a square container under forced vibration in a microgravity environment. Governing equations are solved and the shape of bubbles is captured simultaneously to study interaction between shape and translational motion as well as bubble-bubble interaction.

## METHODOLOGY

Equations governing the motion of bubbles in a liquid domain are the mass and momentum conservation equations,

$$\nabla \cdot \vec{V} = 0 \quad (1)$$

$$\frac{\partial \vec{V}}{\partial t} + \vec{V} \cdot \nabla \vec{V} = -\frac{1}{\rho} \nabla p + \frac{1}{\rho} \nabla \cdot \vec{\tau} + \vec{G} + \frac{1}{\rho} \vec{F}_b \quad (2)$$

where  $\vec{V}$  is the velocity vector,  $p$  the pressure,  $\rho$  the density,  $\tau$  the shear stress,  $\vec{G}$  the gravity, and  $\vec{F}_b$  includes any body force per unit volume. In a vibrating cell the body force oscillates in time ( $\vec{F}_b = \rho \vec{g}_0 \cos(2\pi vt)$ ) where  $g_0$  and  $v$  are the forcing amplitude and frequency, respectively. Therefore there is an oscillatory-time dependent buoyancy force on the bubble. This force is asymmetric around the bubbles and leads to an oscillatory translational motion of the bubbles and at the same time causes shape oscillation.

The numerical scheme developed by Bussmann et al. [7] was employed to solve the above governing equations. These equations are solved on a fixed Cartesian grid. In this scheme both fluids are assumed to be incompressible. By the incompressibility assumption, shape oscillation of the bubble is captured while the bubble volume remains unchanged. The VOF method is used to capture the interface between two phases. This method assumes that there is a scalar field,  $f$ , called volume fraction that is defined at each computational cell as,

$$\begin{cases} f = 1 & \text{within the liquid} \\ 0 < f < 1 & \text{cells with interface} \\ f = 0 & \text{within the gas} \end{cases}$$

The method developed by Youngs [8] is used to reconstruct the interface at each time step and advect volume fractions by the following equation,

$$\frac{\partial f}{\partial t} + (\vec{V} \cdot \nabla) f = 0 \quad (3)$$

Surface tension force is applied using a balanced-force algorithm as [9],

$$\vec{F}_{ST} = \sigma \kappa (\nabla f) \quad (4)$$

where  $\sigma$  is the surface tension,  $\kappa$  is the surface curvature and  $\nabla f$  is the face gradient of the volume fraction field. Equations (1), (2), and (3) are discretized using a staggered mesh in which velocities are specified at cell faces and pressure and volume fraction at each cell center. While the scheme is three-dimensional and viscous, this work presents inviscid two-dimensional results, assuming only one computational cell in one of the three coordinate directions.

## MODEL VALIDATION

In this section results from the numerical model are compared to available experimental data. As mentioned in the introduction, previous studies on forced vibration of bubbles in microgravity have focused on the behavior of a single bubble. Experimental data used here are from the work of Friesen et al. [10]. In their work, a large air bubble with a radius of 2.62 cm was located in a container with dimensions of 10 cm × 10 cm × 2 cm. The front and side views of the setup are shown below.

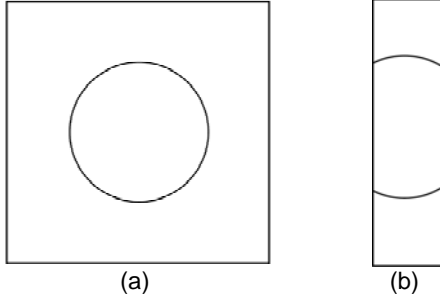


**Figure 1:** experimental setup, (a) front view, (b) side view

Outer fluid was a water-surfactant solution with a density of  $996 \text{ kg/m}^3$  and the fluid inside the bubble was air with a density of  $1.12 \text{ kg/m}^3$ . The surface tension coefficient was  $\sigma = 0.022 \text{ N/m}$ . The container was vibrated in the vertical direction with frequency of  $0.6 \text{ Hz}$ , and the effect of container amplitude,  $A_c$ , on bubble amplitude,  $A_b$ , was examined. Figure 2 illustrates the experimental data as well as numerical results obtained employing the model described in the previous section. Both experimental and numerical results suggest a linear variation between bubble and cell amplitudes. Numerical results predict  $A_b$  to be larger than the corresponding experimental value. The difference is interpreted as the effect of the inviscid assumption and two-dimensional modeling. In the experimental setup, the walls, between which the bubble was sandwiched, and fluid the viscosities would reduce the amplitude of the bubble.

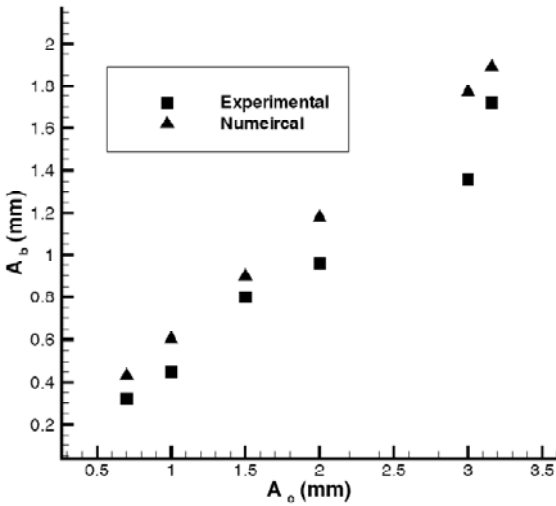


**Figure 2:** comparison of experimental and numerical results

## RESULTS

The interaction of two bubbles in a square vibrating container was studied. The dimensions of the container are  $20 \text{ mm}$  by  $20 \text{ mm}$ . Both bubbles have a radius of  $2 \text{ mm}$ . The configuration of the problem is shown in Fig. 3 (a). The separation between centers of two bubbles,  $d$ , is equal to  $8 \text{ mm}$ . The liquid and gas densities are  $\rho_l$  and  $\rho_g$ , respectively. The container is vibrated in the vertical direction with an amplitude of  $A_c$  and frequency of  $\nu$ . Therefore, the induced acceleration is calculated at each time as,  $F_b/\rho = A_c(2\pi\nu)^2 \cos(2\pi\nu t)$ . In all cases presented here, two bubbles move in an oscillatory trajectory in the vertical direction while interacting with each other and this interaction results in the attraction of bubbles. In addition, shape of the bubbles change depending on the level of acceleration applied. At higher accelerations, nonlinear behavior appears. The shape change affects the forces acting on and consequently the translational motion of the bubbles. Because of the symmetry in the geometry, only the left half of the domain was solved and presented in results. Figure 3 (b) illustrates the boundary conditions applied on this half. In all the results presented, mesh resolution was 16 computational cells per bubble radius.

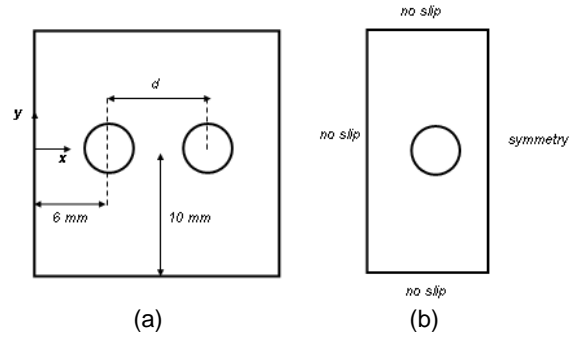


**Figure 3:** (a) schematic of the problem, (b) domain and boundary conditions

### Frequency Effect

This section demonstrates the effect of frequency on the flow field and time required for the collision of bubbles. Two different frequencies are studied,  $\nu = 50$ , and  $100 \text{ Hz}$ . In this section  $\rho_l = 1000 \text{ kg/m}^3$ ,  $\rho_g = 1 \text{ kg/m}^3$ ,  $\sigma = 0.073 \text{ N/m}$ , and  $A_c = 0.1 \text{ mm}$ . Figure 4 (a) demonstrates the position of the bubble in the vertical direction for the two frequencies. In both cases, the bubble oscillates with the same frequency as the container. In addition to the oscillatory motion, a net drift is observed in each case. As the bubble undergoes one period of oscillation a flow field is formed around and inside the bubble and its shape

deviates slightly from its initial circular state. At the end of first oscillation, developed flow field is not identical to the initial condition, which was zero velocity everywhere. Consequently, the second oscillation starts with a different initial condition (velocity and shape) compared to that of the first oscillation. This difference in initial conditions while applying the same body force during each oscillation, results in a transient behavior of the bubbles. As mentioned in the Introduction, this drift was also reported in previous studies as the effect of adjacent solid boundaries, which is present in this study as well. Figure 4 (b) illustrates the position of the center of mass of the left bubble in the horizontal direction for two frequencies. For each frequency, as time passes, the bubble approaches the symmetry boundary (the two bubbles get closer in the full domain) and collision occurs. Elapsed time before collision decreases as frequency increases.

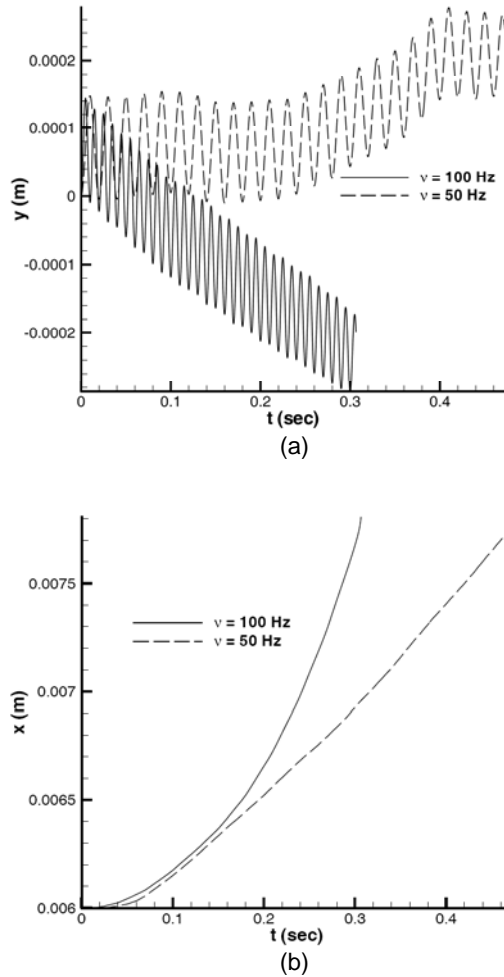


**Figure 4:** (a) position of the bubble in the y-direction, (b) position of the bubble in the x-direction

To demonstrate the effect of frequency on the flow field developed for each case, Figures 5 and 6 illustrate the vertical velocity ( $W$ ) and pressure gradient in the horizontal direction ( $dp/dx$ ) at certain times for each case. As the frequency increases (larger acceleration), higher vertical velocities are observed resulting in stronger pressure gradient fields. The asymmetry in the pressure gradient field drives the bubbles toward each other.

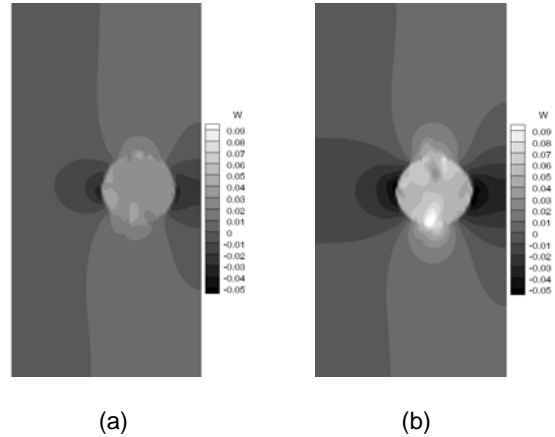


**Figure 5:** contours of vertical velocity in m/s after 12.25 time period, (a)  $\nu = 50$  Hz, (b)  $\nu = 100$  Hz

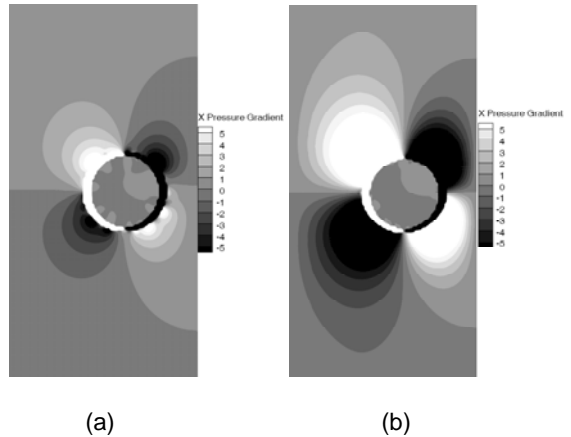


**Figure 6:** contours of pressure gradient in Pa/mm at  $t=0.1$  sec, (a)  $\nu = 50$  Hz, (b)  $\nu = 100$  Hz

### Container Amplitude Effect

In this section, the effect of container amplitude on the bubble behavior is demonstrated. Two different  $A_c$  are tested,  $0.1$  mm,  $0.2$  mm. Vibration frequency is  $100$  Hz and fluid properties are the same as in the previous section. Figure 7 demonstrates the shape of bubbles in certain times for two amplitudes. In this figure,  $T$  is equal to the inverse of the vibration frequency. In the case of  $A_c = 0.1$  mm, the bubble retains its circular shape with small oscillations to oblate and prolate shapes. In the case of  $A_c = 0.2$  mm, the bubble deforms greatly. As the shape of the

bubble changes, inertia and pressure forces acting on it change as well, affecting the translational motion of the bubble as well as its shape. If the amplitude is increased to  $0.4 \text{ mm}$  bubbles breakup before colliding.

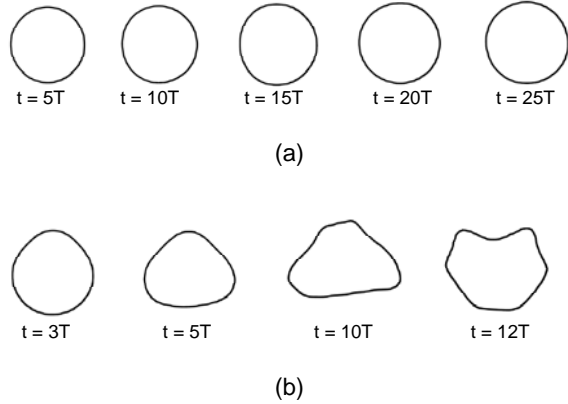


**Figure 7:** shape of the bubble, (a)  $A_c = 0.1 \text{ mm}$ , (b)  $A_c = 0.2 \text{ mm}$

Figure 8 illustrates the position of bubbles in the vertical and horizontal directions for each case. For  $A_c = 0.2 \text{ mm}$  some jumps are observed in the vertical direction compared to the case of  $A_c = 0.1 \text{ mm}$ . These jumps reflect the effect of the shape of the bubble on its center of mass. Similar to the previous section, collision occurs faster at higher accelerations (higher amplitudes).

### Density Ratio Effect

The effect of density ratio on the behavior of bubbles is presented in this section. Four ratios are considered,  $\rho_l / \rho_g = 1000/1, 1000/2, 1000/10, 1000/100$ . Vibration frequency and amplitude are  $100 \text{ Hz}$  and  $0.2 \text{ mm}$ , respectively. Surface tension is kept constant,  $0.073 \text{ N/m}$  for all cases. Outer fluid density is kept fixed while the density of the lighter fluid is changed. Figure 9 demonstrates the effect of density ratio on the bubble amplitude and the time elapsed before collision. As density ratio decreases, the buoyancy force on the bubble decreases resulting in smaller bubble amplitudes. As well, the time required for bubbles to collide increases. In Fig. 9, R and T represent bubble radius and oscillation period, respectively. In all the cases bubbles show large deformations from the circular shape. Bubble amplitude is calculated based on the half of the maximum displacement of the bubble in the first oscillation where its shape is closest to the circular shape.

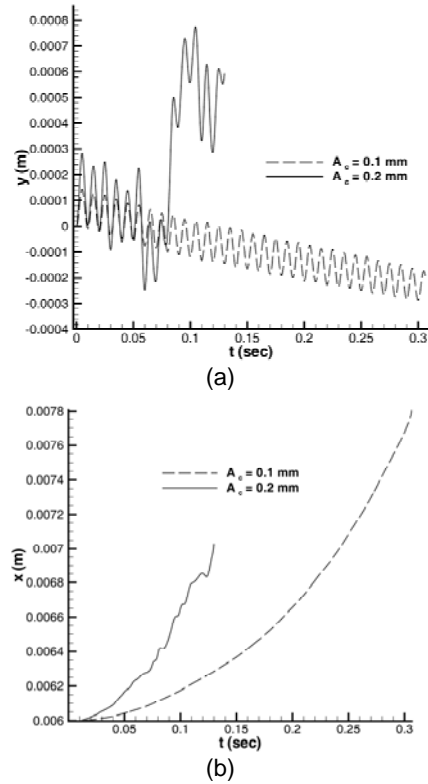


**Figure 8:** (a) position of the bubble in the y-direction, (b) position of the bubble in the x-direction

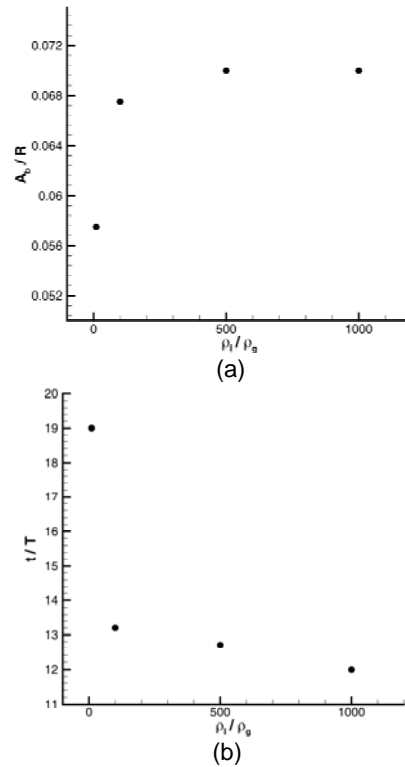


**Figure 9:** effect of density ratio on (a) bubble amplitude, (b) collision time

## Frequency-Amplitude Map

As mentioned earlier, as a result of forced vibration, three bubble behaviors are observed regarding the shape of the bubbles in response to the imposed acceleration; small oscillation, deformation, and breakup. The following map illustrates the effect of vibration frequency and amplitude on the shape and behavior of bubbles. As frequency gets larger while keeping the container amplitude constant, bubble goes from small oscillations to deformation and then to the breakup zone. Similarly, increasing amplitude in a fixed frequency shows the same trend. In both cases, the acceleration is increasing, demonstrating the effect of applied acceleration on the bubble shape and behavior.

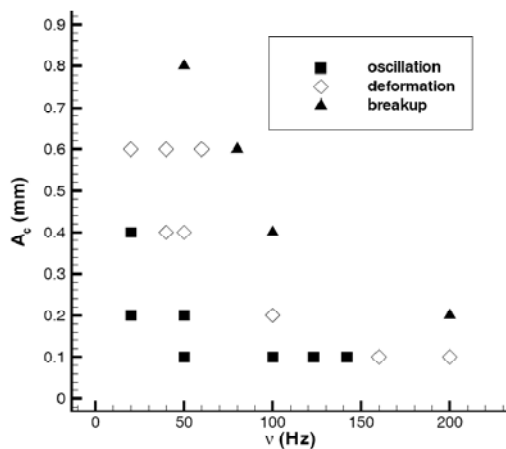


Figure 10: Effect of frequency-amplitude vibration on the shape of the bubble

## SUMMARY

Two-dimensional numerical simulation of a pair of bubbles under forced vibration is studied in the absence of gravity. As a result of the oscillatory applied acceleration, a time dependent buoyancy force is induced on bubbles resulting in an oscillatory translational motion. As bubbles move, shape deformation occurs which, in turn, affects the pressure distribution around the bubbles and forces acting on them. Pressure fields formed around two bubbles interact with each other resulting in bubble attraction and collision. As the vibration frequency and amplitude increase, stronger pressure fields are formed and collision occurs faster. It is shown that at higher liquid to gas density ratios, bubble collision occurs faster and also the amplitude of the translational motion of bubbles with respect to the container increases. Three types of behavior for bubble shapes are identified depending on the imposed acceleration. At small accelerations, small shape oscillations are observed while in higher

accelerations bubbles deform completely from the initial circular shape. At large accelerations, breakup happens before collision of bubbles.

## ACKNOWLEDGMENTS

This work was supported by Canadian Space Agency Space Science Enhancement Program grant 07SCISEP06.

## NOMENCLATURE

A	amplitude
F	force
G	gravity
V	velocity
f	volume fraction
p	pressure
t	time
$\rho$	density
$\kappa$	curvature
$\sigma$	surface tension coefficient
$\tau$	shear stress
$\nu$	frequency
<b>subscript</b>	
ST	surface tension
b	bubble
c	container
g	gas
l	liquid

## REFERENCES

1. Eller, A., Crum, L., 1970, "Instability of the Motion of a Pulsating Bubble in a Sound Field," *J. Acoust. Soc. Am.*, **47**, pp. 762-767.
2. Akhatov, I., Konovalova, S., 2005, "Regular and Chaotic Dynamics of a Spherical Bubble," *J. App. Math. and Mech.*, **69**, pp. 575-584.
3. Bjerknes, V., 1906, *Fields of Force*, Columbia University Press.
4. Brennen, C., 1995, *Cavitation and Bubble Dynamics*, Oxford University Press.
5. Barbat, T., Ashgriz, N., Liu, C., 1999, "Dynamics of Two Interacting Bubbles in Acoustic Fields," *J. Fluid Mech.*, **389**, pp. 137-168.
6. Friesen, T., 2000, "A Numerical Investigation of Large Bubble Translation Behavior due to Forced Vibration under Microgravity," M.A.Sc. Thesis, Department of Chemical Engineering and Applied Chemistry, University of Toronto, Toronto, ON.
7. Bussmann, M., Mostaghimi, J., Chandra, S., 1999, "On a Three Dimensional Volume

- Tracking Model of Droplet Impact,” *Phys. Fluids*, **11**, pp. 1408-1417.
8. Youngs, D. L., 1984, “An Interface Tracking Method for a 3D Eulerian Hydrodynamics Code,” Technical Report 44/92/35, AWRE.
  9. Francois, M., Cummins, S., Dendy, E., Kothe, D., Sicilian, J., Williams, M., 2006, “A Balanced-force Algorithm for Continuous and Sharp Interfacial Surface Tension Models within a Volume Tracking Framework,” *J. Comput. Phys.*, **213**, pp. 141-173.
  10. Friesen, T., Takahira, H., Allegro, L., Yasuda, Y., Kawaji, M., 2002, “Numerical Simulation of Bubble Motion in a Vibrated Cell under Microgravity Using Level Set and VOF Algorithms,” *Ann. N.Y. Acad. Sci.*, **974**, pp. 288-305.